HIV-1 Nucleocapsid Traps Reverse Transcriptase on Nucleic Acid Substrates[†]

Dina Grohmann,[‡,§] Julien Godet,[||] Yves Mély,[||] Jean-Luc Darlix,[⊥] and Tobias Restle*[,‡]

Institut Gilbert Laustriat, Photophysique des interactions moléculaires, UMR 7175 CNRS, Faculté de Pharmacie, Université Louis Pasteur, Strasbourg 1, 74, Route du Rhin, 67401 Illkirch, France, LaboRetro, INSERM 758, IFR 128, ENS de Lyon, 46 Allée d'Italie, 69364 Lyon, France, and Institut für Molekulare Medizin, Universitätsklinikum Schleswig-Holstein, Universität zu Lübeck, Ratzeburger Allee 160, 23538 Lübeck, Germany

Received July 24, 2008; Revised Manuscript Received September 21, 2008

ABSTRACT: Conversion of the genomic RNA of human immunodeficiency virus (HIV) into full-length viral DNA is a complex multistep reaction catalyzed by the reverse transcriptase (RT). Numerous studies have shown that the viral nucleocapsid (NC) protein has a vital impact on various steps during reverse transcription, which is crucial for virus infection. However, the exact molecular details are poorly defined. Here, we analyzed the effect of NC on RT-catalyzed single-turnover, single-nucleotide incorporation using different nucleic acid substrates. In the presence of NC, we observed an increase in the amplitude of primer extension of up to 3-fold, whereas the transient rate of nucleotide incorporation (k_{pol}) dropped by up to 50-fold. To unravel the underlying molecular mechanism, we carefully analyzed the effect of NC on RT−nucleic acid substrate dissociation. The studies revealed that NC considerably enhances the stability of RT−substrate complexes by reducing the observed dissociation rate constants, which more than compensates for the observed drop in k_{pol}. In conclusion, our data strongly support the concept that NC not only indirectly assists the reverse transcription process by its nucleic acid chaperoning activity but also positively affects the RT-catalyzed nucleotide incorporation reaction by increasing polymerase processivity presumably via a physical interaction of the two viral proteins.

The process of reverse transcription during the HIV-1 replication cycle is a complex interplay of different proteins and nucleic acid intermediates. Among these, the reverse transcriptase (RT) is first and foremost responsible for the conversion of the viral RNA into full-length viral DNA. Interestingly, the nucleocapsid protein (NC) chaperones this complex multistep process at the levels of primer tRNA annealing to the PBS (primer binding site) and of the two obligatory DNA strand transfers to generate the long terminal repeats (LTRs) (for reviews, see refs *1*−*4*). NC is synthesized as part of the Gag precursor and subsequently cleaved by the viral protease into polypeptides of 55 and 72 amino acids. The exact biological function of these two forms is poorly understood, though the predominant form of NC found in mature HIV-1 particles mainly consists of 55 amino acids (*5*, *6* and references therein). NC is composed of two zinc fingers flanked by basic residues and is able to bind nucleic acids in a specific (e.g., stem loops SL2 and SL3 of the genomic Psi packaging signal) and nonspecific way. NMR studies of NC/SL−RNA complexes revealed that hydrophobic residues within the zinc fingers interact with the single-stranded loop region of the RNA, while the N-terminal basic domain of the protein undergoes electrostatic interactions with the double-stranded stem region of the RNA (*7*−*9*). NC assists the folding of nucleic acid molecules into their most stable conformation, a property termed nucleic acid chaperoning activity (*10*−*12*). The chaperone activity of NC is comprised of two properties: destabilization of nucleic acid interactions and the ability to promote annealing. The first one is specific, being dependent mainly on the folded fingers, while the second one is less specific and depends for the most part on positively charged residues (*13*−*14*). Due to its ability to destabilize and re-form base pairs, NC participates in a wide range of steps during replication, including the annealing of the $tRNA^{Lys3}$ primer to the viral RNA (*15*−*18*), strand transfer reactions (*19*−*23*), and packaging of the viral genome (*24*−*25*). NC allows efficient polymerization on RT pausing sites (*19*, *26*−*28*), regions within the viral RNA genome that expose secondary structure elements. Moreover, NC has also been shown to enhance the RNase H activity of RT and to protect the full-length viral DNA LTR ends (*1*, *29*−*31*). However, for the most part, the molecular mechanisms of these binding and chaperoning activities are still poorly understood and to a certain extent quite puzzling. Besides its general nucleic acid binding and chaperoning activity, there are some hints that a physical interaction between RT and NC might play a role in facilitating reverse transcription (*32*−*33*).

Numerous detailed transient kinetic as well as structural studies have considerably improved our understanding of the complex interplay of RT with the different nucleic acid

[†] This work was supported in part by ANRS grants to J.-L.D. and Y.M. T.R. acknowledges funding by EC Grant LSHG-CT-2003-503480.

* To whom correspondence should be addressed. Telephone: +49-451-500-2745. Fax: +49-451-500-2729. E-mail: restle@imm.uni-luebeck.de.

[‡] Universität zu Lübeck.

[§] Present address: Institute of Structural and Molecular Biology (ISMB), Division of Biosciences, Faculty of Life Sciences, University College London, Darwin Building, Gower Street, London WC1E 6BT, United Kingdom.

[||] Université Louis Pasteur.

[⊥] INSERM 758, IFR 128.

10.1021/bi801386r CCC: $40.75
Published on Web 10/24/2008

Scheme 1: (A) Minimal Kinetic Model of RT−p/t Interaction and Nucleotide Incorporation and (B) Illustrating Cartoon Based on Pre-Steady-State Kinetic and Single-Molecule Fluorescence Data (*36, 37*)[a]

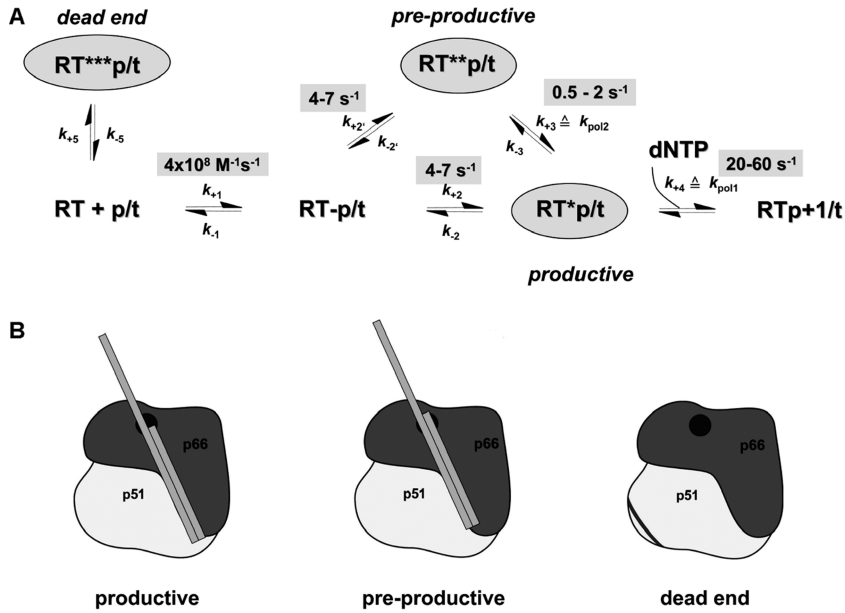

[a] (A) Three distinct RT−primer/template complexes are formed: a productive complex that is capable of nucleotide incorporation, a preproductive complex which has to undergo a conformational change to incorporate nucleotides, and, additionally, a dead-end complex incapable of nucleotide incorporation. The latter can incorporate nucleotide only upon dissociation followed by re-association. The rate constants k_{+1}, k_{+2}, $k_{+2'}$, and k_{+3} for RT−p/t association were determined by stopped flow analysis (*36*). Additionally, monitoring of p/t binding via nucleotide incorporation, k_{+2}, $k_{+2'}$, and k_{+3}, could be confirmed independently by performing quench flow experiments (*36*). k_{+3} and k_{+4} are the rate-limiting steps of nucleotide incorporation (termed k_{pol2} and k_{pol1}) of the preproductive and productive complex, respectively. At present, no firmly established data concerning an assignment of individual rate constants are available for the back reactions. One, two, and three asterisks distinguish structural states of the system that otherwise have the same composition. (B) The productive complex interacts with the p/t (gray bars) in a state closely resembling known X-ray structures (*60, 61*). In the preproductive complex, the primer terminus is shifted such that it now occupies the dNTP-binding pocket (dark circle in p66). For the dead-end complex, the dark line in p51 shows the area of contact of the 5′-terminus of the primer with the protein.

substrates encountered during reverse transcription and the subsequent polymerization reaction (for a comprehensive review, see ref *34*). Previously, we showed that pre-steady-state single-turnover, single-nucleotide incorporation by HIV-1 RT occurs in a biphasic burst followed by a linear phase. This was eventually interpreted on the basis of three different RT−primer/template (p/t) substrate complexes, i.e., a productive enzyme−substrate complex which is capable of nucleotide incorporation and a preproductive complex which has to undergo an isomerization before dNTP incorporation can occur (*35*−*37*). The linear part represents the steady-state phase and is due to a catalytically incompetent dead end complex. In this case, dissociation of RT from the faulty bound nucleic acid substrate followed by proper rebinding is necessary to enable nucleotide incorporation (see Scheme 1 for an illustration). On the basis of these results, we investigated the effect of NC on transient RT-catalyzed single-turnover, single-nucleotide incorporation.

Here we present a further piece of a puzzle along the way to understanding how NC facilitates the process of HIV-1 reverse transcription. The data presented clearly show that NC extends the lifetime of RT−nucleic acid complexes, which in turn affects the processivity of the viral polymerase.

MATERIALS AND METHODS

Proteins. Recombinant, heterodimeric wild-type HIV-1_{BH10} RT was expressed in *Escherichia coli* cells and purified as described previously (*38*). The expression system and purification protocol allowed the preparation of large quantities of the heterodimeric enzyme in a homogeneous form. Furthermore, an RT mutant containing a single accessible cysteine at position 287 of the p66 subunit was used (*39*). This cysteine, situated within the thumb subdomain of p66, was labeled with the green donor fluorophore $Alexa^{488}$-C5 maleimide (*37*). Highly pure NC protein [amino acids 1−55 (NC^{1-55})] was prepared by chemical synthesis as described by de Rocquigny and colleagues (*40*). Lyophilized protein powder (1−2 mg) was first dissolved in 200−400 μL of freshly degassed water at a pH value of ~3 to maintain the thiol groups in a reduced state followed by the addition of zinc sulfate (3 molar equiv) and adjustment of the pH to 7.5 with 50 mM Hepes buffer. Proteins were stored at −80 °C. Protein concentrations were determined using extinction coefficients at 280 nm of 260450 M^{-1} cm^{-1} (HIV-1 RT) and 5500 M^{-1} cm^{-1} (NC^{1-55}).

Buffers. Unless noted otherwise, all experiments were routinely carried out at 25 °C in a buffer containing 50 mM Tris-HCl (pH 8.0), 50 mM KCl, and 10 mM $MgCl_2$ (standard RT buffer). Nucleic acid annealing buffer consisted of 20 mM Tris-HCl (pH 7.5) and 50 mM NaCl.

Synthetic Oligonucleotides. PAGE-purified oligodeoxynucleotides were purchased from IBA (Göttingen, Germany). Concentrations were determined by UV absorbance at 260 nm. The 18- and 36-mer DNA/DNA primer/template (p/t) (linear substrate) sequences were 5′-TCC CTG TTC GGG CGC CAC and 5′-TGT GGA AAA TCT CTA GAC GTG GCG CCC GAA CAG GGA, respectively. The complementary region is equivalent to the primer binding site (PBS) of

HIV-1. The 20- and 48-mer DNA/DNA p/t (hairpin substrate) sequences were 5′-TCT GCT CTG AAG AAA ATT CC and 5′-ATC TGG CCT TCC TAC AAA GGA AGG CCA GGG AAT TTT CTT CAG AGC AGA, respectively. The sequence is derived from the HIV-1 RNA genome and forms a secondary structure with a stem of 10 bp and a loop of six nucleotides (*41*). The abasic site substrate had the following sequence: template, 5′-AAA TCA XCC TAT CCT CCT TCA GGA CCA ACG TAC; and primer, 5′-CGT TGG TCC TGA AGG AGG ATA GGA. Before annealing, DNA primers were ^{32}P-labeled with T4 polynucleotide kinase at the 5′ end as described previously (*42*).

FRET measurements were carried out with either a Cy5-labeled 19-mer (5′-TTG TCC CTG TTC GGG CGC C) or a 20-mer primer complementary to the 36- and 48-mer, respectively, described above. In both cases, the dye was covalently attached via a C6 amino link to the 5′ end of the corresponding primer strand. Primer and template oligodeoxynucleotides were annealed by heating equimolar amounts in annealing buffer at 90 °C for 2 min, followed by cooling to room temperature over several hours in a heating block. To ensure complete annealing, the hybrids were analyzed by nondenaturing gel electrophoresis.

Gel Retardation Assay. Radioactively labeled substrate (100 nM) was incubated with NC at different molar ratios (see the corresponding Supporting Information figure legend) for 10 min at 25 °C. Next gel loading buffer (20% ficoll, 0.1% bromophenol blue, and 0.1% xylene cyanol) was added, and the samples were analyzed by nondenaturing gel electrophoresis (8% PAA) at 4 °C and subsequent phosphorimaging (Typhoon 8600, GE Healthcare).

Analysis of NC Chaperone Activity. The nucleic acid destabilizing activity of NC was characterized using a doubly labeled cTAR oligonucleotide (5′-GGT TCC TTG CTA GCC AGA GAG CTC CCG GGC TCG ACC TGG TCT AAC AAG AGA GAC C) with 6-carboxyrhodamine (Rh6G) attached to the 5′ end and the quencher DABCYL to the 3′ end (*43*). Experiments were performed in the standard buffer [50 mM Tris-HCl (pH 8.0), 50 mM KCl, and 10 mM $MgCl_2$] and in NC binding buffer [25 mM Tris-HCl (pH 7.5), 30 mM NaCl, and 200 μM $MgCl_2$] using a FluoroMax-3 spectrofluorometer (Horiba Jobin Yvon) with a thermostated cuvette holder at 25 °C in a 600 μL quartz cuvette. Excitation was performed at 480 nm with a 5 nm slit, and emission spectra were recorded from 500 to 700 nm with a 5 nm slit. cTAR (100 nM) was mixed with 1.1 μM NC and incubated for 5 min prior to the emission spectrum being recorded. The NC preparations were judged as active if the quotient of the fluorescence at the emission maximum (550 nm) in the presence and absence of NC was between 6.5 and 7.5 (Figure 1).

NC-mediated annealing of cTAR/dTAR was monitored as described previously (*22*). Briefly, the kinetic measurements were performed under pseudo-first-order conditions by using unlabeled dTAR at a concentration which was at least 10-fold higher than the concentration of cTAR labeled with carboxytetramethylrhodamine (TMR) at the 5′ end and with 5(and 6)-carboxyfluorescein (Fl) at the 3′ end (*44*). Excitation and emission wavelengths were 480 and 520 nm, respectively, for monitoring the Fl fluorescence. NC was added to each oligonucleotide separately at a protein:nucleotide ratio of 2. Mixing the NC-coated oligonucleotides started the annealing reaction. Experiments were performed in 50 mM Tris-HCl (pH 8.0) and 50 mM KCl with either 0.2 or 10 mM $MgCl_2$ at 20 °C. Emission spectra and kinetic traces were recorded with a Fluorolog spectrofluorometer (Jobin Yvon) equipped with a thermostated cell compartment. All fluorescence intensities were corrected for buffer emission and lamp fluctuations.

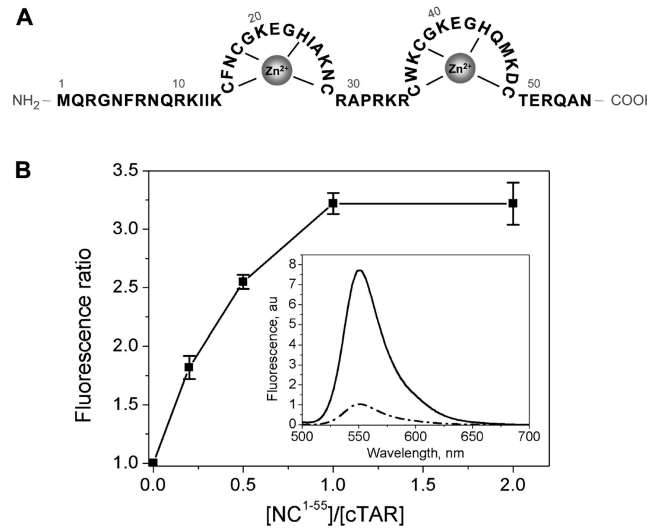

FIGURE 1: Structure and nucleic acid destabilization activity of HIV-1 nucleocapsid protein. (A) Amino acid sequence of HIV-1 NC^{1-55} and coordination of zinc ions within the two zinc fingers. (B) NC-induced destabilization of cTAR. The destabilization of 0.1 μM doubly labeled Rh6G-5′-cTAR-3′-DABCYL in the standard buffer [50 mM Tris-HCl (pH 8.0), 50 mM KCl, and 10 mM $MgCl_2$] was monitored at increasing NC:nucleotide ratios. Error bars are for three independent experiments. The inset shows emission spectra of 0.1 μM Rh6G-5′-cTAR-3′-DABCYL in the absence (−•−) and presence (—) of HIV-1 NC (1.1 μM). The spectra were recorded in 25 mM Tris-HCl (pH 7.5), 30 mM NaCl, and 200 μM $MgCl_2$. Excitation was at 480 nm.

RT−Nucleic Acid Hairpin Substrate Binding. Binding affinities of RT−hairpin substrate complexes were determined by competitive fluorescence titrations (i.e., displacing a fluorescently labeled 5′-FAM-18/36-mer DNA/DNA p/t bound to RT) using a FluoroMax-3 spectrofluorometer. To monitor the fluorescence change upon displacement of the labeled p/t from RT, the samples were excited at 492 nm, and the emission intensity was measured at 516 nm. The competitive titration was evaluated using Scientist (MicroMath Scientific Software), which allows the user to define the system under investigation as a series of parallel equations defining (in this case) each discrete equilibrium, the relationship between the total and free concentrations of the components, and the way in which the observable signal is generated. The K_d of the 18/36-mer DNA/DNA p/t was independently determined (*45*) and kept constant during the fit procedure.

Amplitude of Primer Extension after Single-Turnover, Single-Nucleotide Incorporation. HIV-1 RT was preincubated with radiolabeled p/t substrates for 5 min at 25 °C to allow complex formation. In the case of experiments where NC was present, it was added next and an additional incubation step of 5 min was performed to enable the formation of RT−substrate/NC complexes. The polymerization reaction was started by the addition of the next correct nucleotide to be incorporated (final concentration of 250 μM), and samples were incubated at 25 °C. To ensure single-

turnover conditions and prevent RT of multiple rounds of nucleotide incorporation, a large excess (25 μM) of an anti-RT pseudoknot RNA aptamer (*46, 47; see Figures 4 and 5 of the Supporting Information* for further details) was added together with the nucleotide. Finally, reactions were stopped at different times in the second to minute range by addition of trifluoroacetic acid (TFA, 0.6% final concentration). The samples were mixed with formamide loading buffer, and the elongation of the primer was analyzed by denaturing PAGE. Data were quantified by phosphorimaging.

Rapid Kinetics of Nucleotide Incorporation. Rapid quench experiments were carried out in a chemical quench flow apparatus (RQF-3, KinTek Corp.). Reactions were started by rapidly mixing the reactants [RT−substrate complexes in the presence or absence of NC with nucleotide and RNA aptamer trap (*46, 47*), 15 μL each] and then quenched with 0.6% TFA at defined time intervals in the millisecond to second range. All concentrations reported are final concentrations after mixing in the rapid quench apparatus. Products were analyzed by denaturing gel electrophoresis (10% polyacrylamide and 7 M urea in TBE buffer) and quantified by scanning the dried gel using a phosphor imager. The experimental data were fitted to the double-exponential equation [product] = $A[1 - \exp(-k_{pol1}t)] + B[1 - \exp(-k_{pol2}t)]$ using Grafit (Erithacus Software). *A* and *B* are the amplitudes of the biphasic burst, which reflects the concentration of catalytically competent p/t-bound enzyme at time zero. The effective pre-steady-state constants (k_{pol1} and k_{pol2}) are derived from the exponential rates.

Analysis of RT−Nucleic Acid Substrate Dissociation in the Presence of NC by Fluorescence Resonance Energy Transfer (FRET) Measurements. RT−nucleic acid substrate dissociation was followed using a FRET system described previously (*37, 39; see Figure 6 of the Supporting Information* for further details). Briefly, the p66 subunit of the HIV-1 RT was site specifically labeled with the donor fluorophore Alexa^{488} at position 287. The acceptor fluorophore Cy5 was introduced at the 5′ end of a 19-mer (linear substrate) or 20-mer (hairpin substrate) primer annealed to the corresponding template oligonucleotide (see Synthetic Oligonucleotides). Formation of RT−substrate complexes results in fluorescence energy transfer from Alexa^{488} to Cy5.

All measurements were taken at 25 °C using a Fluoro-Max-3 spectrofluorometer and a 70 μL fluorescence cuvette (Hellma). Excitation of the labeled RT was performed at 493 nm, and the FRET signal was recorded at 670 nm (in both cases with a 1 nm slit). As described above for the nucleotide incorporation experiments, preincubation of RT and substrate was followed by a second incubation step with NC. Next, the sample was rapidly mixed with a competitor solution containing the anti-HIV-1 RT RNA aptamer at 25 μM (*47*), which prevents a rebinding of the primer/template motifs to RT. Time-resolved measurements of the change in the FRET signal after addition of the competitor solution allowed the calculation of dissociation rate constants using a double- or triple-exponential equation.

RESULTS

Nucleic Acid Binding and Chaperoning Properties of HIV-1 NC Protein. In this study, chemically synthesized nucleocapsid protein consisting of 55 (NC$^{1-55}$) amino acids

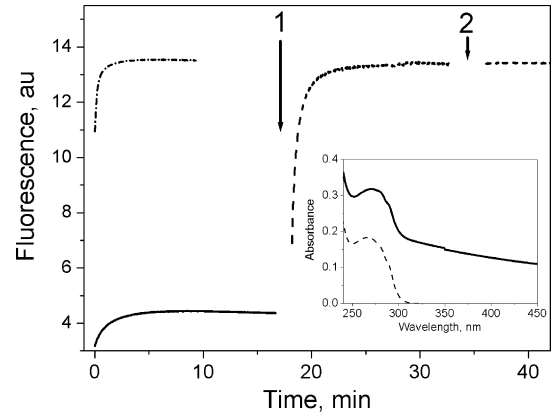

FIGURE 2: Effect of the Mg^{2+} concentration on NC-induced cTAR−dTAR annealing and aggregation (see Figure 2 of the Supporting Information for further details). The annealing kinetics of 0.1 μM TMR-5′-cTAR-3′-Fl with 2 μM dTAR in the presence of NC at a protein:nucleotide ratio of 2 were monitored in 50 mM Tris-HCl (pH 8.0), 50 mM KCl, and either 0.2 mM (—) or 10 mM $MgCl_2$ (-•-). At low Mg^{2+} concentrations, the fluorescence increase was limited. At the time indicated by arrow 1, the concentration of Mg^{2+} was increased to 10 mM, leading to a full restoration of the fluorescence emission. A further increase in the Mg^{2+} concentration to 20 mM at the time indicated by arrow 2 did not further affect the fluorescence emission. Excitation and emission wavelengths were 480 and 520 nm, respectively. The inset shows absorption spectra. The absorption spectrum recorded at 0.2 mM Mg^{2+} (—) shows a strong light scattering, indicative of aggregation. Addition of 10 mM Mg^{2+} fully suppresses the light scattering (---), suggesting that aggregates dissociated.

was used (Figure 1A). First, the NC preparations were tested in terms of chaperoning activities to control the functionality of the protein preparations. Experiments were initially performed in 25 mM Tris-HCl (pH 7.5), 30 mM NaCl, and 200 μM $MgCl_2$, where NC chaperone properties are optimal (*15*). A fluorescently labeled cTAR oligonucleotide which folds into a stem loop structure was used as described by Bernacchi and colleagues (*43*). Here the fluorescence of Rh6G attached to the 5′ end of cTAR is quenched by 3′ end-linked DABCYL. Upon addition of active NC, the stem loop structure is partly melted, resulting in a separation of the labeled termini and subsequently in an increase in fluorescence. An increase of a factor of 6.5−7.5-fold was seen (Figure 1B, inset), indicating chaperoning competent, fully active, and folded NC (*13*). Only active NC preparations were used in subsequent studies.

In a next step, the nucleic acid binding capability of NC in the standard buffer [50 mM Tris-HCl (pH 8.0), 50 mM KCl, and 10 mM $MgCl_2$] used for the RT assays described below was investigated using gel retardation electrophoresis. Radioactively labeled RT−nucleic acid substrates (termed linear or hairpin substrate; see Figure 3), which later were used for nucleotide incorporation experiments (see below), were mixed with increasing amounts of NC. In both cases, a concentration-dependent gel shift of the primer/template substrates, linear as well as hairpin substrate, was observed with complete retardation only at a NC:nucleotide molar ratio of 5:1 (Figure 1 of the Supporting Information). This high molar ratio suggests that the affinity of NC for nucleic acids is rather low in the standard buffer. This is likely due to the high Mg^{2+} concentration (10 mM), since an increase in the Mg^{2+} concentration from 1 to 10 mM was previously shown to decrease the affinity of NC for its target oligonucleotides by 2 orders of magnitude (*48*).

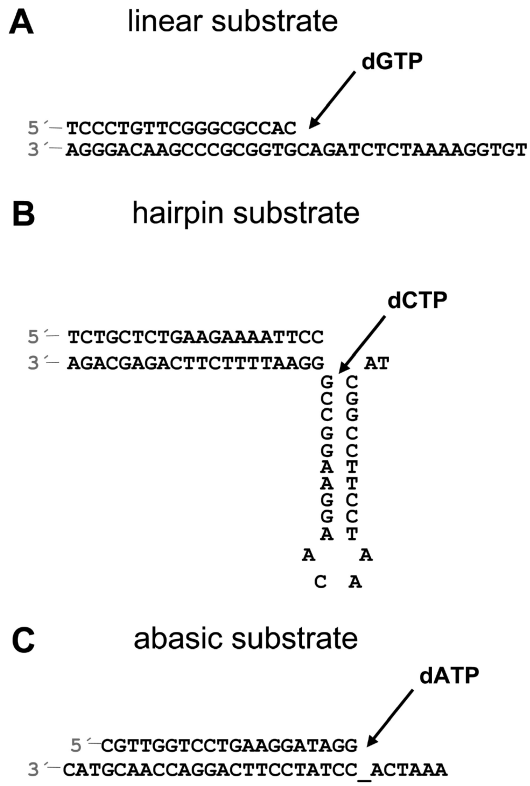

FIGURE 3: Sequences of the different DNA/DNA p/t substrates used in this study. For panels A and B, the next correct nucleotide to be incorporated is shown.

Next, we checked whether the chaperone properties of NC were preserved in the standard buffer used for the enzymatic RT assays. At a NC:nucleotide ratio of 0.2, which induces optimal destabilization of cTAR at low Mg^{2+} concentrations, only a 1.8-fold fluorescence increase was observed (Figure 1B). By increasing the NC concentration, we found that the NC-induced destabilization of cTAR reached a plateau which corresponded to a 3.3-fold fluorescence increase at a NC:nucleotide ratio of 1. Both the limited fluorescence increase and the shift toward high NC:nucleotide ratios likely result from the decreased affinity of NC for cTAR and the increased stability of cTAR at 10 mM Mg^{2+} (*43, 48*).

To further characterize the NC chaperone properties in the standard RT buffer, we investigated NC-induced cTAR−dTAR annealing. This reaction was monitored in real time, after the weakly fluorescent TMR-5′-cTAR-3′-Fl had been mixed with an excess of nonlabeled dTAR in the presence of NC at a protein:nucleotide ratio of 2. A rapid fluorescence increase was observed that reached a plateau in less than 5 min (Figure 2), instead of several hours in the absence of NC. The increase in fluorescence was identical to the situation in which formation of the cTAR−dTAR duplex was achieved when the samples were heated (*49*), which strongly suggests that the reaction went to completion (Figure 2 of the Supporting Information). Thus, NC efficiently chaperones the cTAR−dTAR annealing reaction even at high Mg^{2+} concentrations.

In sharp contrast to the experiments performed at high Mg^{2+} concentrations, at 0.2 mM Mg^{2+} we observed a limited fluorescence increase (Figure 2) as well as strong light scattering in the absorption spectrum (Figure 2, inset) unambiguously indicative of strong aggregation under these conditions (*22*). However, addition of 10 mM Mg^{2+} to these aggregates led to a fast fluorescence increase that reached the same fluorescence level in less than 30 min as the heat-induced cTAR−dTAR duplexes. Moreover, the light scattering in the absorption spectrum completely disappeared, indicating that 10 mM Mg^{2+} led to dissociation of the NC−oligonucleotide aggregates. A further increase in the Mg^{2+} concentration to 20 mM did not change the fluorescence, suggesting that dissociation of the aggregates was already complete at 10 mM Mg^{2+}.

Taken together, the results presented above evidently show that NC is fully functional at high Mg^{2+} concentrations given that the molar ratio of protein to nucleotide is increased accordingly, and despite this high ratio, no aggregation occurs. These findings were an indispensable prerequisite for the experiments described in the following sections.

Effect of HIV-1 NC on the Amplitude of RT-Catalyzed Single-Nucleotide Incorporation. To assess whether the NC protein affects HIV-1 RT-catalyzed single-turnover, single-nucleotide incorporation, the amplitude of primer extension (i.e., the percentage of primers extended by one or more nucleotides) was analyzed. To ensure that these experiments were performed under saturating conditions of nucleic acid substrate and incoming nucleotide (including Mg^{2+}), the binding equilibria of the binary (RT−p/t) and ternary (RT−p/t−nucleotide) complexes needed to be known. Binding affinities of RT for the kind of linear DNA/DNA p/t substrate used in this study (Figure 3) and such a complex for the incoming nucleotide were determined in previous studies (*35*) with K_d values of approximately 2 nM and 10 μM, respectively. The affinity of RT for the hairpin substrate was determined via competitive titrations by displacing a fluorescently labeled 5′-FAM-18/36-mer DNA/DNA p/t substrate bound to the enzyme, resulting in a K_d of 83 ± 14 nM (Figure 3 of the Supporting Information). Accordingly, RT concentrations were increased from 100 nM to 2 μM when with the hairpin substrate was used to ensure complete substrate binding. RT was premixed with either of the two substrates to allow formation of a binary complex before NC was added to this solution. The polymerase reaction was started with the next correct nucleotide to be incorporated in the presence of a trap [anti-HIV-1 RT 33 nt pseudoknot RNA aptamer (Figure 4 of the Supporting Information)]. This trap shows an affinity for RT of <25 pM, which is ~100-fold stronger than for the linear substrate, and was shown in the past to very effectively block multiple-turnover events without affecting substrate-bound RT (refs *36* and *47* and Figure 5 of the Supporting Information).

Polymerization products were separated on a denaturing gel as shown in Figure 4A for the hairpin substrate. It is already evident from simple examination of the gel that the bands corresponding to the elongated primer became more abundant. Figure 4B shows a quantitative analysis of the effect of NC on RT-catalyzed single-turnover, single-nucleotide primer extension using three different nucleic acid substrates [linear, hairpin, and abasic site substrate (see Figure 3)]. Additionally, misincorporation of dTTP (opposite template nt C at position +1) into the linear substrate is shown.

In the case of the linear substrate, we observed a 3-fold enhanced incorporation of dGTP at position primer+2 (in this case misincorporation opposite template nt A), whereas primer+1 extension (opposite template nt C) remained

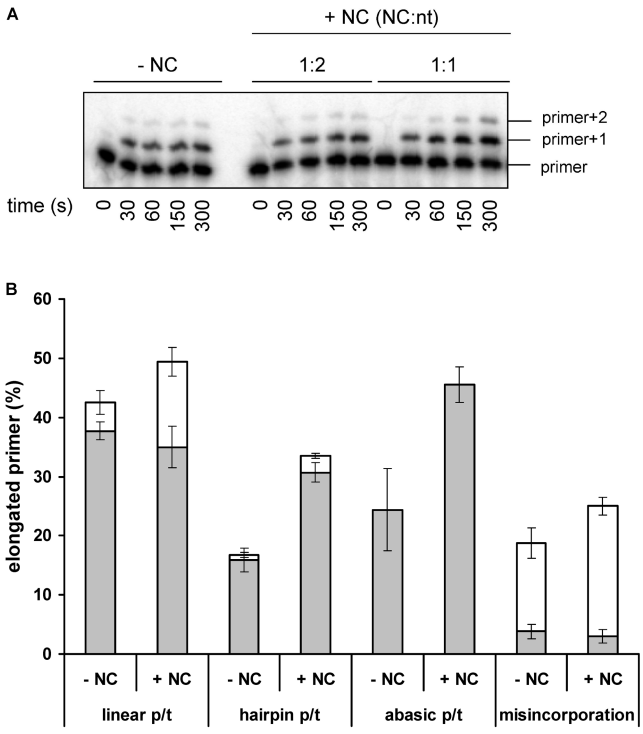

FIGURE 4: Effect of NC on the amplitude of RT-catalyzed single-turnover, single-nucleotide incorporation. For single-nucleotide incorporation experiments, 100 nM radiolabeled substrates [linear, hairpin, and abasic site substrate (see Figure 3)] were preincubated with HIV-1 RT (100 nM in the case of the linear substrate and 2 μM in the case of the hairpin substrate) followed by a second preincubation step with HIV-1 NC. The polymerization reaction was started by addition of nucleotide (250 μM dGTP, dCTP, and dATP in the cases of linear, hairpin, and abasic site substrate, respectively, and 2 mM dTTP in the case of misincorporation into the linear substrate) and 25 μM anti-HIV-1 RT RNA aptamer as a competitor to prevent multiple-turnover events (see Figures 4 and 5 of the Supporting Information for further details). The elongation of the primer was analyzed by denaturing PAGE and quantified by phosphorimaging. In panel A, the polymerization products at different incubation times of RT−hairpin substrate complexes with different NC concentrations (1:2 molar ratio, 3.4 μM NC; 1:1 molar ratio, 6.8 μM NC) are shown. (B) Amplitudes of different primer extensions after incubation for 5 min. The relative distribution of primer+1 (gray bars) and primer+2 (white bars) products in the absence or presence of HIV-1 NC (NC:nucleotide ratio of 2:1) is shown. Details are given in the text. Results were obtained from three independent experiments each. The standard deviation is given by the error bars.

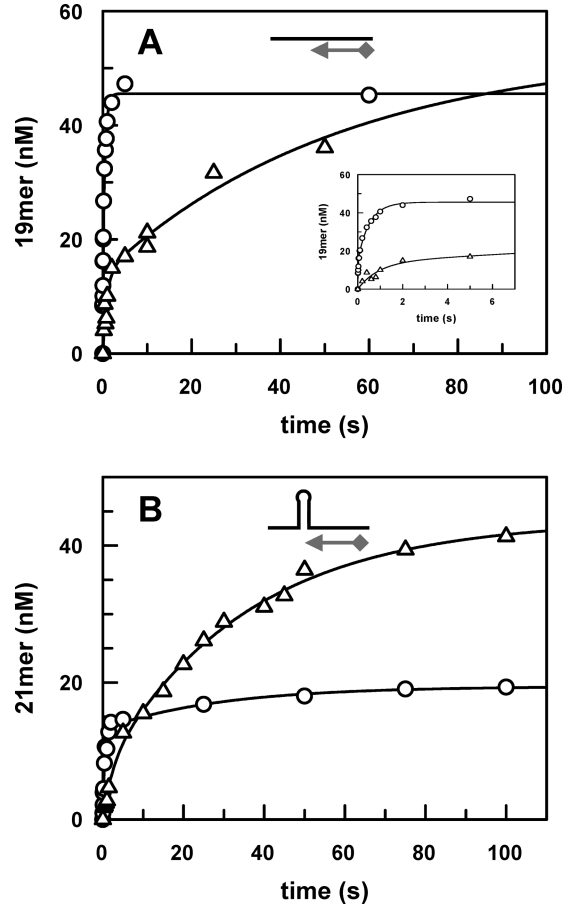

FIGURE 5: Rapid kinetics of single-turnover, single-nucleotide incorporation into linear or hairpin DNA/DNA p/t (see Figure 3) by HIV-1 RT. A preformed complex of 100 nM (A, linear substrate) or 2 μM (B, hairpin substrate) RT and 100 nM p/t in the absence (○) or presence (△) of HIV-1 NC (NC:nucleotide ratio of 2:1) was rapidly mixed with either 250 μM dGTP (A) or dCTP (B) and 25 μM anti HIV-1 RT RNA aptamer (see Figures 4 and 5 of the Supporting Information for further details). The curves show the best fit of the data to a double-exponential equation yielding k_{pol1} and k_{pol2} values of 56 ± 12 and 1.9 ± 0.2 s^{-1}, and 2.3 ± 0.3 and 0.03 ± 0.01 s^{-1} for the linear and hairpin substrate, respectively, in the absence of NC. In the presence of NC, we observed rates of 1.1 ± 0.3 and 0.02 ± 0.03 s^{-1}, and 0.4 ± 0.2 and 0.03 ± 0.003 s^{-1}, for the linear and hairpin substrate, respectively. The inset shows the reaction on a shorter time scale. Data are summarized in Table 1.

largely unaffected. RT-catalyzed incorporation of dCTP into the hairpin substrate in the presence of NC affected both amplitudes (primer+1/template nt G and primer+2/template nt A) which increased by 2- and 3-fold, respectively. In line with the dependence of NC chaperone activity on the NC:nucleotide ratio (Figure 1B), a ratio of 2:1 yielded the best results. Choosing higher or lower NC:nucleotide ratios led to a reduction of the observed effect (data not shown). Furthermore, we were also interested in whether NC is able to promote misincorporation at position primer+1 and to facilitate incorporation opposite abasic template sites. Misincorporation of dTTP opposite template nt C using the same linear substrate that was used previously was only slightly but significantly enhanced by a factor of 1.5 for primer+2 extension, which essentially reflects incorporation at position primer+1 as position+2 corresponds to correct incorporation and should therefore be much faster than the preceding step. Incorporation of dATP in the presence of NC into a substrate with an abasic site at template position+1 resulted in an increase in the level of primer+1 extension of 1.9-fold, whereas no incorporation at position primer+2 could be observed.

Influence of NC on the Transient Polymerization Rate of HIV-1 RT. Next we analyzed the effect of NC on the pre-steady-state, single-nucleotide incorporation rate. Again, preformed RT−substrate complexes in the presence or absence of NC were rapidly mixed with the incoming nucleotide together with the aptamer trap, and the polymerase reaction was monitored in the millisecond to second range using a quench flow apparatus (Figure 5). As briefly outlined in the introductory section and previously described in detail (*36, 37*), single-turnover, single-nucleotide incorporation by HIV-1 RT occurs under such experimental conditions with a biphasic exponential burst where the sum of the amplitudes of the burst is equivalent to the amount of

Table 1: Summary of the Effects of NC on the HIV-1 RT-Catalyzed Rate of Single-Nucleotide Incorporation and RT−p/t Dissociation[a]

substrate	NC	k_{pol1} (s^{-1})	k_{pol2} (s^{-1})	k_{diss1} (s^{-1})	k_{diss2} (s^{-1})	k_{diss3} (s^{-1})
linear	−	56 ± 12 (15)	1.9 ± 0.2 (30)	3 ± 0.14 (67)	0.24 ± 0.006 (24)	−
linear	+	1.1 ± 0.3 (14)	0.02 ± 0.03 (40)	0.04 ± 0.0006 (46)	0.006 ± 0.0001 (30)	−
hairpin	−	2.3 ± 0.3 (13)	0.03 ± 0.01 (6)	2.4 ± 0.08 (62)	0.5 ± 0.02 (20)	0.04 ± 0.0005 (12)
hairpin	+	0.4 ± 0.2 (7)	0.03 ± 0.003 (37)	0.17 ± 0.002 (87)	0.02 ± 0.002 (6)	−

[a] The numbers in parentheses show the distribution of the different amplitudes (given in nanomolar for k_{pol} and in arbitrary fluorescence units for k_{diss}). The corresponding experiments are shown in Figures 5 and 6. Refer to Scheme 1 for an overview of how the numbers given above are related to the minimal kinetic model of RT−p/t interaction and nucleotide incorporation. As outlined in the text, due to the complexity of the system, it is currently not possible to precisely assign k_{diss1}, k_{diss2}, and k_{diss3} to individual steps for the backward reaction given in Scheme 1 (i.e., k_{-1}, k_{-2}, $k_{-2'}$, k_{-3}, and k_{-5}).

catalytically competent p/t-bound enzyme at the start of the reaction and the rates of nucleotide incorporation are given by the exponential terms (Figure 5 of the Supporting Information). With the linear substrate, we observed incorporation rates (k_{pol1} and k_{pol2}) of 56 ± 12 and 1.9 ± 0.2 s^{-1}, respectively, highly consistent with previous findings (*35, 36, 50*). On the other hand, the hairpin substrate exhibited substantially slower incorporation rates of 2.3 ± 0.3 and 0.03 ± 0.01 s^{-1}, respectively, consistent with a study by Suo and Johnson (*41*). Upon addition of NC, the pre-steady-state nucleotide incorporation rates in the case of the linear substrate dropped dramatically to 1.1 ± 0.3 and 0.02 ± 0.03 s^{-1}, respectively, while for incorporation into the hairpin substrate, only the faster rate was reduced by a factor of ~6 with the slower rate being unaffected. Moreover, for the linear substrate, the amplitude of nucleotide incorporation (sum of the two burst phases) remained largely unaffected by NC, whereas we observed a more than 2-fold increase in the case of the hairpin sequence, consistent with the findings described above for the primer extension studies. Data are summarized in Table 1.

Effect of NC on the Stability of the RT−Substrate Complex. In the preceding sections, we could show that NC causes an increase in the amplitude of primer extension and at the same time a reduction of the rate of nucleotide incorporation. A rational explanation for this finding could be a NC-mediated increased stability of RT−nucleic acid complexes. For this reason, we investigated RT−nucleic acid complex dissociation. Analyzing a given protein−nucleic acid interaction in the context of a second nucleic acid binding protein is a challenging task since a differentiation of the two proteins in terms of substrate binding is technically difficult. To resolve this problem, we applied a FRET-based system enabling us to exclusively observe RT−nucleic acid interactions (Figure 6 of the Supporting Information). Here, the FRET signal of Cy5, a fluorophore attached to the 5′ end of the primer molecule, is a direct measure of the number of RT−substrate complexes as the transfer of energy from the donor fluorophore Alexa^{488} attached to the thumb domain of RT is only possible within a RT−nucleic acid complex. Preformed RT−nucleic acid substrate complexes (linear or hairpin substrate) in the presence or absence of NC were rapidly mixed with an excess of competitor (Figure 6; see Table 1 for a summary). Analysis of the dissociation process of the RT−linear substrate complex revealed two phases with dissociation rate constants (k_{diss1} and k_{diss2}) of 3 ± 0.14 and 0.24 ± 0.006 s^{-1}, respectively. The presence of NC considerably decelerated dissociation of the complex. Here dissociation rate constants of 0.04 ± 0.0006 and 0.006 ± 0.0001 s^{-1} were observed. Similar data were determined with the hairpin substrate. However, in contrast to the linear substrate data, these data best fit an equation with three exponentials giving rates of 2.4 ± 0.08, 0.5 ± 0.02, and 0.04 ± 0.0005 s^{-1} in the absence of NC and 0.17 ± 0.002 and 0.02 ± 0.002 s^{-1} in the presence of NC. In the latter case, data were fitted to a double-exponential equation. Appropriate control experiments showed that the Alexa^{488} label at position 287 did not significantly alter the kinetic parameters of RT (refs *51* and *52* and unpublished data of T. Restle).

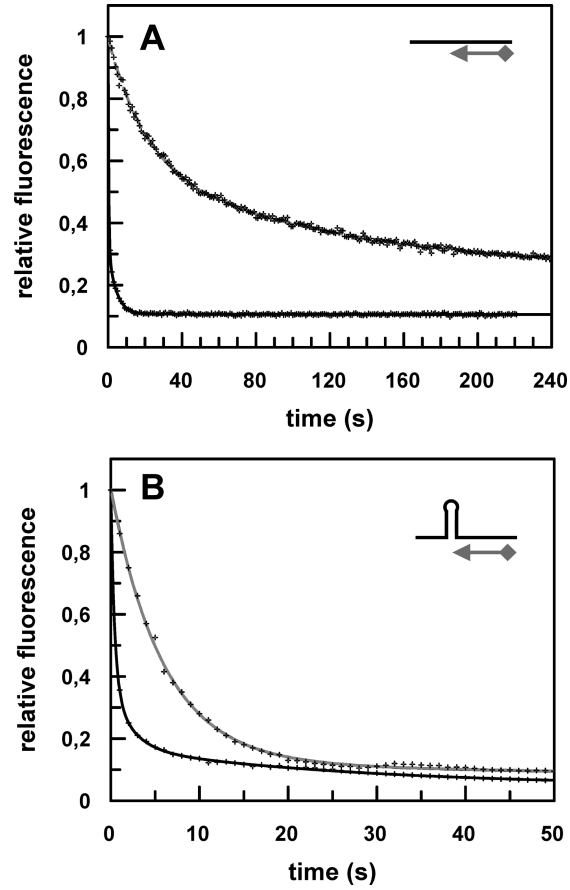

FIGURE 6: FRET measurements of RT−p/t dissociation kinetics. (A) Linear 5′-Cy5-p/t (100 nM) was preincubated with 100 nM HIV-1 RT^{A488} (see Figure 6 of the Supporting Information for a graphical illustration) and rapidly mixed with 25 μM aptamer competitor in the absence (black curve) or presence (gray curve) of NC (10.8 μM). (B) Dissociation of RT (2 μM) from 100 nM hairpin p/t after being mixed with 25 μM RNA aptamer in the absence (black curve) or presence (gray curve) of NC (13.6 μM). Data were fitted to a double- or triple-exponential equation. The corresponding rates and amplitudes are given in Table 1.

DISCUSSION

Over the years, many studies provided evidence that NC assists tRNA annealing, reverse transcription initiation,

minus-strand transfer, processivity of reverse transcription, plus-strand transfer, strand displacement synthesis, and moreover 3′ processing of viral DNA by integrase, and integrase-mediated strand transfer (for recent reviews, see refs *3* and *4*). It seems rather peculiar that such a small protein can affect so many seemingly different processes. Interestingly, all these essential viral reactions involve protein−nucleic acid interactions, and NC may act as a "macromolecular crowding" factor to enhance the stability and activity of such RNA and DNA replicating complexes (*1, 3, 4, 53*). However, in most cases, the molecular details of this facilitator activity remain poorly understood. The aim of this study was to explore possible effects of HIV-1 NC on RT-catalyzed single-turnover, single-nucleotide incorporation applying pre-steady-state techniques and to unravel some of the underlying mechanistic characteristics.

In a first set of kinetic experiments, we analyzed the effect of NC on the amplitude of single-nucleotide primer extension under strict single-turnover conditions. Depending on the nucleic acid substrate (linear, hairpin, or abasic site DNA/DNA primer/template, i.e., p/t), an increase in the level of extended primers by a factor of 1.5−3 was observed with the distribution of primers elongated by one or two nucleotides varying considerably. It should be noted that extension of the primers by more than one nucleotide reflects misincorporation as the experimental setup as well as the sequences was designed to allow the incorporation of one single Watson−Crick base-paired nucleotide. In all but one case, NC considerably affected the apparent nucleotide incorporation fidelity of RT. Interestingly, with a substrate containing an abasic site at template position +1, we observed only primer+1 extension, albeit at a level increased by a factor of ∼1.9 in the presence of NC, which would indicate that the orientation of the 3′ end of the primer in the active site of the polymerase is highly unfavorable to allow for the incorporation of a second mismatched nucleotide. As a first approximation, one would have expected an effect of NC in the case of the hairpin substrate due to a destabilization of its stable stem structure caused by the NC chaperoning activity. However, our results with the linear p/t substrate clearly show the stimulating effect of NC is not restricted to those kinds of substrates.

Maximal stimulation of primer extension was detected at a NC:nucleotide molar ratio of 2:1. As in the virion, the viral RNA is coated with NC proteins at an approximate ratio of 1:7 (*48, 54, 55*), and the concentration of NC necessary to stimulate the polymerization reaction and to achieve full retardation of the p/t substrates in the gel shift assay (Figure 1 of the Supporting Information) was rather high. This finding most likely was due to the $MgCl_2$ concentration of 10 mM that was used. High concentrations (i.e., >1 mM) of this divalent cation have been shown to considerably reduce the level of NC binding to nucleic acids (*48, 56*). Along these lines, Anthony et al. described similar observations, where the production of long-range DNAs was stimulated only at high NC concentrations (*57*). These results are in excellent agreement with NC chaperoning assays performed at 10 mM $MgCl_2$ shown in Figures 1B and 2. For NC-mediated nucleic acid destabilization as well as annealing under high-$MgCl_2$ conditions, we also had to use a protein:nucleotide ratio of ∼2:1 to reach maximal activity. In contrast, at low $MgCl_2$ concentrations (i.e., 0.2 mM), full activity has already been observed at a NC:nucleotide ratio of 0.2:1. Now one could argue that the nucleotide incorporation experiments should be performed under more physiologically relevant concentrations (i.e., <1 mM). To ensure that the single-turnover rate of nucleotide incorporation observed is limited by internal rate-limiting kinetic parameters, rather than by binding parameters for p/t, dNTP, and $MgCl_2$, which occurs when concentrations below the saturation level are used, we were forced to use such high concentrations of $MgCl_2$. Moreover, in all previously conducted experiments regarding single-turnover nucleotide incorporation, we used a concentration of this divalent cation of 10 mM. Accordingly, we would not have been able to relate the data of this study with the comprehensive data sets derived before concerning a kinetic model of the complex RT-catalyzed nucleotide incorporation reaction (*35*−*37*). For this matter, it was essential for this study to show that NC is active even at 10 mM $MgCl_2$, albeit at a much higher protein:nucleotide ratio, but does not induce any aggregation of the nucleic acid substrate (Figure 2).

Next we analyzed the transient rate (k_{pol}) of single-nucleotide incorporation in the presence of NC. As briefly outlined in the introductory section, incorporation of a nucleotide by HIV-1 RT is a complicated process, which involves at least three conformationally distinct enzyme−nucleic acid complexes (Scheme 1). As a consequence, one observes a biphasic burst of nucleotide incorporation with an amplitude of considerably less than 100% due to the formation of dead-end complexes, although under the chosen experimental conditions one theoretically would expect a single burst of product formation with an amplitude corresponding to the amount of active enzyme present at the start of the reaction (*36*). Our studies revealed that the presence of NC decreased the rate of fast pre-steady-state nucleotide incorporation (k_{pol1}) of RT by up to 50-fold (linear substrate) and was most likely due to NC molecules, which completely cover the substrate and in this way hinder translocation of the enzyme along the nucleic acid. The decrease of the second slow phase (k_{pol2}) by a factor of ∼90 is even more pronounced. This nicely fits the model of two catalytically competent RT−p/t complexes, as the second complex has to translocate from a product to an educt state before incorporation can occur (i.e., the educt state is a complex in which the nucleic acid is positioned to allow nucleotide incorporation, whereas the product state is formed immediately after nucleotide incorporation but before RT translates to the next nucleotide). In the case of the hairpin substrate, the situation is different. Here two effects of NC might outweigh each other, so in the end k_{pol1} is decreased by only ∼6-fold. It is likely that the hampering effect of NC is compensated by a destabilization of the hairpin structure, which in turn would accelerate nucleotide incorporation. The second slow phase is already so slow that it remained unaffected by NC. Another interesting aspect is the observed shift in the relative distribution of the two burst phases. While there is only a slight reduction in the amplitude of the fast phase from 33 to 26% (amplitude of the fast phase relative to the sum of two amplitudes) in the case of the linear substrate, the hairpin p/t shows a dramatic reduction in the percentage of this phase from 68 to 15% (Table 1). This indicates that NC might have an effect on the relative distribution of the two different catalytically competent RT-p/t complexes [i.e., preproductive and productive enzyme−substrate complexes (Scheme 1)].

Two opposing effects are caused by NC: an increase in the amplitude of primer extension on one hand and a drastically reduced transient rate of nucleotide incorporation on the other. How does this fit together? A rather simple explanation would be an enhanced stability of the enzyme−substrate complexes, which would compensate for the reduced rate of a catalytic or precatalytic step and consequently increased processivity. To address this question, we performed experiments to analyze the RT−nucleic acid substrate dissociation process (Table 1). For this purpose, we applied an established FRET-based system (*37, 39*), which enabled us to exclusively observe RT−p/t complexes. For the dissociation of RT from a DNA/DNA p/t substrate, we detected two or three phases with distinct rates of k_{diss1}, k_{diss2}, and k_{diss3} consistent with previous work (ref *36* and unpublished data of T. Restle). Addition of NC to a preformed RT−linear p/t complex reduced the dissociation rate constants (k_{diss1} and k_{diss2}) of the two observed steps by ~75- and ~40-fold, respectively. For the hairpin substrate, we could resolve three phases. Again, we observed considerable reductions of the two fast rates in the presence of NC of approximately 14- and 25-fold, respectively. Deriving precise numbers concerning the degree of deceleration of complex dissociation is not trivial as an exact assignment of the individual phases observed to individual steps (i.e., RT−p/t complexes; also see Scheme 1) is very difficult. However, what can be stated with certainty is that NC substantially increased the stability of RT−nucleic acid complexes, which more than compensates for the reduction of k_{pol} and thus overall leads to an increase in processivity. Recently, Bampi et al. described an analogous observation (*58*). Here in the presence of NC^{1-71} an approximately 16-fold reduction in the apparent dissociation rate constant (from 0.059 to 0.0036 s^{-1}) was determined indirectly by performing steady-state single-nucleotide incorporation measurements. Moreover, they report a more efficient extension of mutated cDNAs with a higher rate of corrected mutations in the presence of NC. Essentially, these observations fit very nicely with our results.

With respect to the underlying molecular mechanism of the NC-mediated stabilization of RT−p/t complexes, we currently can only speculate. One likely scenario would be a direct physical interaction of the two viral proteins (*32*). According to such a model, NC might hold RT onto the nucleic acid substrate. Attempts to map such potential sites of interaction on the polymerase with the help of 23 anti-RT monoclonal antibodies (*59*) (i.e., testing their potential to block the effect of NC on RT−substrate dissociation) have so far never been successful.

In conclusion, our data further contribute to the concept that NC assists RT during viral replication. The observed NC-mediated increase in the lifetime of RT−nucleic acid complexes enhances processivity overall but possibly even more importantly facilitates the overcoming of exceptional situations (e.g., nucleic acid lesions or particular secondary structures) which ultimately ensures synthesis of the full-length viral DNA flanked by the LTR. Furthermore, the proposed physical interplay of the two proteins might offer a promising target for the development of novel antiviral compounds.

ACKNOWLEDGMENT

We thank Hugues de Rocquigny for synthesis of the NC proteins and Francesca Di Pasquale for the abasic site substrate.

SUPPORTING INFORMATION AVAILABLE

Nucleic acid binding properties of HIV-1 NC, emission spectra of TMR-5′-cTAR-3′-Fl, displacement titration of fluorescent p/t bound to RT with the hairpin substrate, structure of the HIV-1 RT−RNA aptamer complex, trap experiments with the RNA aptamer, and the FRET-based system used for RT−nucleic acid complex dissociation experiments. This material is available free of charge via the Internet at http://pubs.acs.org.

REFERENCES

1. Bampi, C., Jacquenet, S., Lener, D., Decimo, D., and Darlix, J. L. (2004) The chaperoning and assistance roles of the HIV-1 nucleocapsid protein in proviral DNA synthesis and maintenance. *Int. J. Biochem. Cell Biol. 36*, 1668–1686.
2. Levin, J. G., Guo, J., Rouzina, I., and Musier-Forsyth, K. (2005) Nucleic acid chaperone activity of HIV-1 nucleocapsid protein: Critical role in reverse transcription and molecular mechanism. *Prog. Nucleic Acid Res. Mol. Biol. 80*, 217–286.
3. Darlix, J. L., Garrido, J. L., Morellet, N., Mely, Y., and de Rocquigny, H. (2007) Properties, functions, and drug targeting of the multifunctional nucleocapsid protein of the human immunodeficiency virus. *Adv. Pharmacol. 55*, 299–346.
4. Thomas, J. A., and Gorelick, R. J. (2008) Nucleocapsid protein function in early infection processes. *Virus Res. 134*, 39–63.
5. Chertova, E., Chertov, O., Coren, L. V., Roser, J. D., Trubey, C. M., Bess, J. W., Jr., Sowder, R. C., Barsov, E., Hood, B. L., Fisher, R. J., Nagashima, K., Conrads, T. P., Veenstra, T. D., Lifson, J. D., and Ott, D. E. (2006) Proteomic and biochemical analysis of purified human immunodeficiency virus type 1 produced from infected monocyte-derived macrophages. *J. Virol. 80*, 9039–9052.
6. Coren, L. V., Thomas, J. A., Chertova, E., Sowder, R. C., Gagliardi, T. D., Gorelick, R. J., and Ott, D. E. (2007) Mutational analysis of the C-terminal gag cleavage sites in human immunodeficiency virus type 1. *J. Virol. 81*, 10047–10054.
7. Morellet, N., Demene, H., Teilleux, V., Huynh-Dinh, T., de Rocquigny, H., Fournie-Zaluski, M. C., and Roques, B. P. (1998) Structure of the complex between the HIV-1 nucleocapsid protein NCp7 and the single-stranded pentanucleotide d(ACGCC). *J. Mol. Biol. 283*, 419–434.
8. De Guzman, R. N., Wu, Z. R., Stalling, C. C., Pappalardo, L., Borer, P. N., and Summers, M. F. (1998) Structure of the HIV-1 nucleocapsid protein bound to the SL3 psi-RNA recognition element. *Science 279*, 384–388.
9. Amarasinghe, G. K., De Guzman, R. N., Turner, R. B., Chancellor, K. J., Wu, Z. R., and Summers, M. F. (2000) NMR structure of the HIV-1 nucleocapsid protein bound to stem-loop SL2 of the psi-RNA packaging signal. Implications for genome recognition. *J. Mol. Biol. 301*, 491–511.
10. Tsuchihashi, Z., and Brown, P. O. (1994) DNA strand exchange and selective DNA annealing promoted by the human immunodeficiency virus type 1 nucleocapsid protein. *J. Virol. 68*, 5863–5870.
11. Darlix, J. L., Lapadat-Tapolsky, M., de Rocquigny, H., and Roques, B. P. (1995) First glimpses at structure-function relationships of the nucleocapsid protein of retroviruses. *J. Mol. Biol. 254*, 523–537.
12. Herschlag, D. (1995) RNA chaperones and the RNA folding problem. *J. Biol. Chem. 270*, 20871–20874.
13. Beltz, H., Clauss, C., Piemont, E., Ficheux, D., Gorelick, R. J., Roques, B., Gabus, C., Darlix, J. L., de Rocquigny, H., and Mely, Y. (2005) Structural determinants of HIV-1 nucleocapsid protein for cTAR DNA binding and destabilization, and correlation with inhibition of self-primed DNA synthesis. *J. Mol. Biol. 348*, 1113–1126.
14. Williams, M. C., Rouzina, I., Wenner, J. R., Gorelick, R. J., Musier-Forsyth, K., and Bloomfield, V. A. (2001) Mechanism for nucleic

acid chaperone activity of HIV-1 nucleocapsid protein revealed by single molecule stretching. *Proc. Natl. Acad. Sci. U.S.A. 98*, 6121–6126.
15. Lapadat-Tapolsky, M., Pernelle, C., Borie, C., and Darlix, J. L. (1995) Analysis of the nucleic acid annealing activities of nucleocapsid protein from HIV-1. *Nucleic Acids Res. 23*, 2434–2441.
16. Li, X., Quan, Y., Arts, E. J., Li, Z., Preston, B. D., de Rocquigny, H., Roques, B. P., Darlix, J. L., Kleiman, L., Parniak, M. A., and Wainberg, M. A. (1996) Human immunodeficiency virus Type 1 nucleocapsid protein (NCp7) directs specific initiation of minus-strand DNA synthesis primed by human tRNA(Lys3) in vitro: Studies of viral RNA molecules mutated in regions that flank the primer binding site. *J. Virol. 70*, 4996–5004.
17. Feng, Y. X., Campbell, S., Harvin, D., Ehresmann, B., Ehresmann, C., and Rein, A. (1999) The human immunodeficiency virus type 1 Gag polyprotein has nucleic acid chaperone activity: Possible role in dimerization of genomic RNA and placement of tRNA on the primer binding site. *J. Virol. 73*, 4251–4256.
18. Hargittai, M. R., Gorelick, R. J., Rouzina, I., and Musier-Forsyth, K. (2004) Mechanistic insights into the kinetics of HIV-1 nucleocapsid protein-facilitated tRNA annealing to the primer binding site. *J. Mol. Biol. 337*, 951–968.
19. Wu, T., Guo, J., Bess, J., Henderson, L. E., and Levin, J. G. (1999) Molecular requirements for human immunodeficiency virus type 1 plus-strand transfer: Analysis in reconstituted and endogenous reverse transcription systems. *J. Virol. 73*, 4794–4805.
20. Johnson, P. E., Turner, R. B., Wu, Z. R., Hairston, L., Guo, J., Levin, J. G., and Summers, M. F. (2000) A mechanism for plus-strand transfer enhancement by the HIV-1 nucleocapsid protein during reverse transcription. *Biochemistry 39*, 9084–9091.
21. Muthuswami, R., Chen, J., Burnett, B. P., Thimmig, R. L., Janjic, N., and McHenry, C. S. (2002) The HIV plus-strand transfer reaction: Determination of replication-competent intermediates and identification of a novel lentiviral element, the primer over-extension sequence. *J. Mol. Biol. 315*, 311–323.
22. Godet, J., de Rocquigny, H., Raja, C., Glasser, N., Ficheux, D., Darlix, J. L., and Mely, Y. (2006) During the early phase of HIV-1 DNA synthesis, nucleocapsid protein directs hybridization of the TAR complementary sequences via the ends of their double-stranded stem. *J. Mol. Biol. 356*, 1180–1192.
23. Ramalanjaona, N., de Rocquigny, H., Millet, A., Ficheux, D., Darlix, J. L., and Mely, Y. (2007) Investigating the mechanism of the nucleocapsid protein chaperoning of the second strand transfer during HIV-1 DNA synthesis. *J. Mol. Biol. 374*, 1041–1053.
24. Berkowitz, R., Fisher, J., and Goff, S. P. (1996) RNA packaging. *Curr. Top. Microbiol. Immunol. 214*, 177–218.
25. D'Souza, V., and Summers, M. F. (2005) How retroviruses select their genomes. *Nat. Rev. Microbiol. 3*, 643–655.
26. Ji, X., Klarmann, G. J., and Preston, B. D. (1996) Effect of human immunodeficiency virus type 1 (HIV-1) nucleocapsid protein on HIV-1 reverse transcriptase activity in vitro. *Biochemistry 35*, 132–143.
27. Drummond, J. E., Mounts, P., Gorelick, R. J., Casas-Finet, J. R., Bosche, W. J., Henderson, L. E., Waters, D. J., and Arthur, L. O. (1997) Wild-type and mutant HIV type 1 nucleocapsid proteins increase the proportion of long cDNA transcripts by viral reverse transcriptase. *AIDS Res. Hum. Retroviruses 13*, 533–543.
28. Klasens, B. I., Huthoff, H. T., Das, A. T., Jeeninga, R. E., and Berkhout, B. (1999) The effect of template RNA structure on elongation by HIV-1 reverse transcriptase. *Biochim. Biophys. Acta 1444*, 355–370.
29. Peliska, J. A., Balasubramanian, S., Giedroc, D. P., and Benkovic, S. J. (1994) Recombinant HIV-1 nucleocapsid protein accelerates HIV-1 reverse transcriptase catalyzed DNA strand transfer reactions and modulates RNase H activity. *Biochemistry 33*, 13817–13823.
30. Chen, Y., Balakrishnan, M., Roques, B. P., and Bambara, R. A. (2003) Steps of the acceptor invasion mechanism for HIV-1 minus strand strong stop transfer. *J. Biol. Chem. 278*, 38368–38375.
31. Roda, R. H., Balakrishnan, M., Hanson, M. N., Wöhrl, B. M., Le Grice, S. F., Roques, B. P., Gorelick, R. J., and Bambara, R. A. (2003) Role of the Reverse Transcriptase, Nucleocapsid Protein, and Template Structure in the Two-step Transfer Mechanism in Retroviral Recombination. *J. Biol. Chem. 278*, 31536–31546.
32. Lener, D., Tanchou, V., Roques, B. P., Le Grice, S. F., and Darlix, J. L. (1998) Involvement of HIV-I nucleocapsid protein in the recruitment of reverse transcriptase into nucleoprotein complexes formed in vitro. *J. Biol. Chem. 273*, 33781–33786.
33. Druillennec, S., Caneparo, A., de Rocquigny, H., and Roques, B. P. (1999) Evidence of interactions between the nucleocapsid protein NCp7 and the reverse transcriptase of HIV-1. *J. Biol. Chem. 274*, 11283–11288.
34. Furman, P. A., Painter, G. R., and Anderson, K. S. (2000) An analysis of the catalytic cycle of HIV-1 reverse transcriptase: Opportunities for chemotherapeutic intervention based on enzyme inhibition. *Curr. Pharm. Des. 6*, 547–567.
35. Thrall, S. H., Krebs, R., Wöhrl, B. M., Cellai, L., Goody, R. S., and Restle, T. (1998) Pre-steady-state kinetic characterization of RNA-primed initiation of transcription by HIV-1 reverse transcriptase and analysis of the transition to a processive DNA-primed polymerization mode. *Biochemistry 37*, 13349–13358.
36. Wöhrl, B. M., Krebs, R., Goody, R. S., and Restle, T. (1999) Refined model for primer/template binding by HIV-1 reverse transcriptase: Pre-steady-state kinetic analyses of primer/template binding and nucleotide incorporation events distinguish between different binding modes depending on the nature of the nucleic acid substrate. *J. Mol. Biol. 292*, 333–344.
37. Rothwell, P. J., Berger, S., Kensch, O., Felekyan, S., Antonik, M., Wöhrl, B. M., Restle, T., Goody, R. S., and Seidel, C. A. (2003) Multiparameter single-molecule fluorescence spectroscopy reveals heterogeneity of HIV-1 reverse transcriptase:primer/template complexes. *Proc. Natl. Acad. Sci. U.S.A. 100*, 1655–1660.
38. Müller, B., Restle, T., Weiss, S., Gautel, M., Sczakiel, G., and Goody, R. S. (1989) Co-expression of the subunits of the heterodimer of HIV-1 reverse transcriptase in *Escherichia coli*. *J. Biol. Chem. 264*, 13975–13978.
39. Kensch, O., Restle, T., Wöhrl, B. M., Goody, R. S., and Steinhoff, H. J. (2000) Temperature-dependent equilibrium between the open and closed conformation of the p66 subunit of HIV-1 reverse transcriptase revealed by site-directed spin labelling. *J. Mol. Biol. 301*, 1029–1039.
40. de Rocquigny, H., Ficheux, D., Gabus, C., Fournie-Zaluski, M. C., Darlix, J. L., and Roques, B. P. (1991) First large scale chemical synthesis of the 72 amino acid HIV-1 nucleocapsid protein NCp7 in an active form. *Biochem. Biophys. Res. Commun. 180*, 1010–1018.
41. Suo, Z., and Johnson, K. A. (1998) DNA secondary structure effects on DNA synthesis catalyzed by HIV-1 reverse transcriptase. *J. Biol. Chem. 273*, 27259–27267.
42. Krebs, R., Immendörfer, U., Thrall, S. H., Wöhrl, B. M., and Goody, R. S. (1997) Single-step kinetics of HIV-1 reverse transcriptase mutants responsible for virus resistance to nucleoside inhibitors zidovudine and 3-TC. *Biochemistry 36*, 10292–10300.
43. Bernacchi, S., Stoylov, S., Piemont, E., Ficheux, D., Roques, B. P., Darlix, J. L., and Mely, Y. (2002) HIV-1 nucleocapsid protein activates transient melting of least stable parts of the secondary structure of TAR and its complementary sequence. *J. Mol. Biol. 317*, 385–399.
44. Beltz, H., Azoulay, J., Bernacchi, S., Clamme, J. P., Ficheux, D., Roques, B., Darlix, J. L., and Mely, Y. (2003) Impact of the terminal bulges of HIV-1 cTAR DNA on its stability and the destabilizing activity of the nucleocapsid protein NCp7. *J. Mol. Biol. 328*, 95–108.
45. Divita, G., Müller, B., Immendörfer, U., Gautel, M., Rittinger, K., Restle, T., and Goody, R. S. (1993) Kinetics of interaction of HIV reverse transcriptase with primer/template. *Biochemistry 32*, 7966–7971.
46. Jaeger, J., Restle, T., and Steitz, T. A. (1998) The structure of HIV-1 reverse transcriptase complexed with an RNA pseudoknot inhibitor. *EMBO J. 17*, 4535–4542.
47. Kensch, O., Connolly, B. A., Steinhoff, H. J., McGregor, A., Goody, R. S., and Restle, T. (2000) HIV-1 reverse transcriptase-pseudoknot RNA aptamer interaction has a binding affinity in the low picomolar range coupled with high specificity. *J. Biol. Chem. 275*, 18271–18278.
48. Mely, Y., de Rocquigny, H., Sorinas-Jimeno, M., Keith, G., Roques, B. P., Marquet, R., and Gerard, D. (1995) Binding of the HIV-1 nucleocapsid protein to the primer tRNA(3Lys), in vitro, is essentially not specific. *J. Biol. Chem. 270*, 1650–1656.
49. Bernacchi, S., Piemont, E., Potier, N., Dorsselaer, A., and Mely, Y. (2003) Excitonic heterodimer formation in an HIV-1 oligonucleotide labeled with a donor-acceptor pair used for fluorescence resonance energy transfer. *Biophys. J. 84*, 643–654.
50. Cramer, J., Strerath, M., Marx, A., and Restle, T. (2002) Exploring the effects of active site constraints on HIV-1 reverse transcriptase DNA polymerase fidelity. *J. Biol. Chem. 277*, 43593–43598.

51. Kensch, O. (2000) Untersuchungen zur Konformation und Dynamik der Reversen Transkriptase von HIV-1 durch ESR- und Einzelmolekülfluoreszenzspektroskopie, Thesis, University of Dortmund, Dortmund, Germany.
52. Rothwell, P. J. (2002) Structural Investigations on HIV-1 RT using single pair Fluorescence Resonance Energy Transfer, Thesis, University of Dortmund, Dortmund, Germany.
53. Jarvis, T. C., Ring, D. M., Daube, S. S., and von Hippel, P. H. (1990) "Macromolecular crowding": Thermodynamic consequences for protein-protein interactions within the T4 DNA replication complex. *J. Biol. Chem. 265*, 15160–15167.
54. Karpel, R. L., Henderson, L. E., and Oroszlan, S. (1987) Interactions of retroviral structural proteins with single-stranded nucleic acids. *J. Biol. Chem. 262*, 4961–4967.
55. You, J. C., and McHenry, C. S. (1993) HIV nucleocapsid protein. Expression in *Escherichia coli*, purification, and characterization. *J. Biol. Chem. 268*, 16519–16527.
56. Wu, T., Heilman-Miller, S. L., and Levin, J. G. (2007) Effects of nucleic acid local structure and magnesium ions on minus-strand transfer mediated by the nucleic acid chaperone activity of HIV-1 nucleocapsid protein. *Nucleic Acids Res. 35*, 3974–3987.
57. Anthony, R. M., and DeStefano, J. J. (2007) In vitro Synthesis of Long DNA Products in Reactions with HIV-RT and Nucleocapsid Protein. *J. Mol. Biol. 365*, 310–324.
58. Bampi, C., Bibillo, A., Wendeler, M., Divita, G., Gorelick, R. J., Le Grice, S. F., and Darlix, J. L. (2006) Nucleotide excision repair and template-independent addition by HIV-1 reverse transcriptase in the presence of nucleocapsid protein. *J. Biol. Chem. 281*, 11736–11743.
59. Restle, T., Pawlita, M., Sczakiel, G., Müller, B., and Goody, R. S. (1992) Structure-function relationships of HIV-1 reverse transcriptase determined using monoclonal antibodies. *J. Biol. Chem. 267*, 14654–14661.
60. Jacobo-Molina, A., Ding, J., Nanni, R. G., Clark, A. D., Jr., Lu, X., Tantillo, C., Williams, R. L., Kamer, G., Ferris, A. L., Clark, P., Hizi, A., Hughes, S. H., and Arnold, E. (1993) Crystal structure of human immunodeficiency virus type 1 reverse transcriptase complexed with double-stranded DNA at 3.0 Å resolution shows bent DNA. *Proc. Natl. Acad. Sci. U.S.A. 90*, 6320–6324.
61. Huang, H., Chopra, R., Verdine, G. L., and Harrison, S. C. (1998) Structure of a Covalently Trapped Catalytic Complex of HIV-1 Reverse Transcriptase: Implications for Drug Resistance. *Science 282*, 1669–1675.

BI801386R